Temporal variations of the $^{18}O/^{16}O$ signal of the whole-canopy transpiration in a temperate forest

Xuhui Lee,[1] Kyounghee Kim,[1] and Ronald Smith[2]

Received 26 October 2006; revised 20 April 2007; accepted 25 June 2007; published 25 August 2007.

[1] Biosphere-atmosphere exchange of water vapor isotopes plays an important role in the global atmospheric ^{18}O-CO_2 and ^{18}O-O_2 budgets. In this paper, we report the results of the first continuous measurements of isotope ratios of water vapor and the evapotranspiration flux in a temperate forest over one full growing season. We found that the $^{18}O/^{16}O$ isotopic signal of the whole-canopy transpiration (δ_T) was not in steady state with respect to plant source water. The departure from steady state was greatest at night and on days of low transpiration rates. Relative humidity was an important driver on timescales shorter than a few hours; on the diurnal timescale, the nonsteady state behavior was driven by relative humidity and the covarying transpiration rate. On average, δ_T was lowest in midmorning and highest at midnight, with an average peak-to-peak variation on the order of 15‰ over the growing season. A diurnal variation of 60‰ or more was observed on some days. On the seasonal timescale, δ_T was tightly coupled with the precipitation isotope ratio in the early growing season and fluctuated around the isotope ratio of the stem water of overstory trees in the late growing season. The temporal shift suggests that the forest switched its water source from the shallow to the deep soil pool and that the overstory trees dominated the whole stand transpiration in the late growing season. Using isotopic partitioning, we estimated that the overstory trees contributed roughly 70% to the whole-stand transpiration water loss during the growing season.

Citation: Lee, X., K. Kim, and R. Smith (2007), Temporal variations of the $^{18}O/^{16}O$ signal of the whole-canopy transpiration in a temperate forest, *Global Biogeochem. Cycles*, *21*, GB3013, doi:10.1029/2006GB002871.

1. Introduction

[2] Oxygen isotopes of water are excellent tracers for the investigation of plant-water relations and water vapor and carbon dioxide exchanges between land vegetation and the atmosphere. It is known that root uptake and transport in the plant do not alter the isotopic composition of water. In leaf tissues, transpiration will result in enrichment of the heavy $H_2{}^{18}O$ isotope. On timescales much greater than the turnover time of water in the leaves, mass balance constraints require that the $^{18}O/^{16}O$ isotopic ratio of the transpired water (δ_T) should be equal to that of the soil water in the rooting zone. On small timescales of minutes to hours, δ_T is variable in field conditions, implying that the steady state assumption (SSA), that δ_T is identical to the isotopic ratio of stem water (δ_S), is in general not satisfied [*Farquhar and Cernusak*, 2005; *Lai et al.*, 2005; *Harwood et al.*, 1998]. At present, little is known about how biotic and abiotic factors influence the temporal variations of δ_T at the ecosystem scale.

[3] An improved understanding of the temporal behavior of δ_T is relevant to several problems in earth and ecological sciences. In the process of transpiration, the enriched leaf ^{18}O signal is passed to the O_2 molecules released by photosynthesis and the CO_2 molecules that diffuse out of the stomatal cavity, thus playing an important role in the budgets of ^{18}O in atmospheric oxygen and carbon dioxide [*Hoffmann et al.*, 2004; *Farquhar et al.*, 1993]. It is also a confounding factor that must be accounted for before proper reconstruction of paleoclimate with plant material, such as lipids, can be made [*Sternberg*, 1988]. How to best quantify the leaf enrichment effect remains an active area of research. It is suggested that it is the $^{18}O/^{16}O$ ratio of water at the evaporating site within the stomatal cavity, $\delta_{L,e}$, not that of the bulk leaf water, δ_L, that exerts direct influences on the ^{18}O-CO_2 and ^{18}O-O_2 exchanges [*Farquhar and Cernusak*, 2005]. However, $\delta_{L,e}$ is not an observable quantity. In the past, researchers have relied on models of varying degrees of sophistication to predict $\delta_{L,e}$ [*Farquhar and Cernusak*, 2005; *Roden and Ehleringer*, 1999; *Flanagan et al.*, 1991; *Dongmann et al.*, 1974]. For the purpose of verification, these model predictions are compared with measurements of δ_L after appropriate corrections for the Peclet effect have been made [*Farquhar and Cernusak*, 2005], or are used in calculations of the photosynthetic discrimination of ^{18}O-CO_2 which are then compared with observations [*Seibt et al.*,

[1]School of Forestry and Environmental Studies, Yale University, New Haven, Connecticut, USA.
[2]Department of Geology and Geophysics, Yale University, New Haven, Connecticut, USA.

0886-6236/07/2006GB002871$12.00

2006; *Cernusak et al.*, 2004]. Obviously, the $\delta_{L,e}$ signal is also passed to δ_T. So far, the coupling between δ_L and δ_T has not been adequately investigated. A good knowledge of the temporal dynamics of δ_T therefore has the potential to improve the $\delta_{L,e}$ predictions, especially if its measurement is made in a nondestructive manner and on a continuous basis.

[4] Observations of the isotopic content of transpiration provide a necessary constraint in order for the whole-stand water vapor flux to be partitioned into its component fluxes using isotope labeling [*Williams et al.*, 2004; *Yakir and Wang*, 1996]. Quantification of the component fluxes, especially the overstory transpiration rate, which is the largest component flux in temperate forests, is of interest because it allows new insights into the causes of the observed temporal and spatial variations in the flux. Absent of the isotopic data, the overstory transpiration rate can be determined by scaling up the sap flow of canopy trees to the whole forest or by measuring the flux both within and above the canopy layer with eddy covariance. The sap flow method is best suited for stands of even-aged single species [*Wilson et al.*, 2001]. The eddy covariance approach works only if there is a clear vertical separation between the understory and overstory canopy layers and the overstory canopy is sufficiently sparse to permit air turbulence inside the stand [*Blanken et al.*, 2001]. The isotopic labeling method can overcome these limitations if data on the isotope ratio of the whole-stand flux are available. Such data can be obtained from the Keeling analysis of the water vapor isotope ratio observed inside the canopy [*Williams et al.*, 2004]. According to *Farquhar and Cernusak* [2005], it is necessary to correct the Keeling parameters for the nonsteady state behavior of the transpired water. Direct measurement of δ_T avoids the necessity of such correction.

[5] A majority of the rich literature on the topic of vapor isotopic exchange has been established from observational studies at the leaf and plant scale [e.g., *Yakir and Sternberg*, 2000]. Several attempts have been made to quantify the isotopic water vapor flux at the canopy scale, by measuring the vertical gradients of vapor concentration and isotope ratio in the surface layer [*Riley et al.*, 2003; *He et al.*, 2001; *Yakir and Wang*, 1996]. While the theory that underlies this experimental method is well-established, its field implementation is hampered by the fact that the vapor isotope ratio gradient often approaches the detection limit of a mass spectrometer. Furthermore, it is extremely labor-intensive to conduct continuous observations at a high temporal frequency (e.g., hourly) with the flask sampling/mass spectrometry method. For these reasons, these published studies are limited to discrete samplings and short durations (usually a few hours). These difficulties were circumvented with the in situ method deployed in this study.

[6] In this paper, we report the results of a field experiment on water vapor flux and its isotope ratio in a temperate forest over one growing season. In the experiment, we deployed a newly developed in situ technique for the measurement of vapor isotope ratio and modified for the micrometeorological flux-gradient application. The objectives of our study were twofold: (1) to quantify how environmental variables influence the temporal variation of the canopy-scale transpiration $^{18}O/^{16}O$ isotope ratio at multiple timescales ranging from hours to season, and (2) to investigate the temporal dynamics of forest water use over the growing season. Our study appears to be the first of its kind in that the isotope observation was made continuously at the canopy scale, at a high temporal resolution, and over one full growing season. Our data offered the opportunity to extend the current knowledge of isotopic water exchange to the ecosystem scale and to increase the realism of future modeling efforts by expanding parameter spaces that are not easily reproducible in a laboratory setting.

2. Theoretical Considerations

[7] The isotopic content of transpiration is a result of complex interplay between relative humidity (h), the vapor isotope ratio (δ_V) and $\delta_{L,e}$, and can be described by the Craig-Gordon equation [*Yakir and Sternberg*, 2000]

$$\delta_T = \left[\alpha_{eq}\delta_{L,e} - h\delta_V - \epsilon_{eq} - (1-h)\epsilon_k\right]/[(1-h)(1+\epsilon_k/1000)], \quad (1)$$

where α_{eq} is the temperature-dependent equilibrium factor, and $\epsilon_{eq} = (1 - \alpha_{eq}) \times 1000$ (‰). The kinetic factor for ^{18}O-H_2O, ϵ_k, is given by

$$\epsilon_k = \frac{32r_s + 21r_b}{r_s + r_b}, \quad \text{‰}$$

where r_s and r_b are stomatal and boundary layer resistance, respectively [*Cernusak et al.*, 2005]. In this study, r_s was not measured. Calculations using the Penman-Monteith big-leaf model showed that r_s was much greater than r_b. In the following, ϵ_k was assumed to be equal to 32‰.

[8] Equation (1) was used to elucidate mechanisms of environmental control on δ_T, both qualitatively, as was done in section 5.1 to isolate the effect of h, and as part of a numerical scheme to achieve a solution of δ_T. In the numerical scheme, equation (1) served as the outflow boundary condition to the ^{18}O mass conservation of the canopy foliage water [*Dongmann et al.*, 1974],

$$dR_L = (R_S - R_T)\frac{F_T}{m}dt, \quad (2)$$

where t is time, R denotes the $^{18}O/^{16}O$ molar ratio, subscripts L, S and T denote leaf, stem and transpiration, respectively, F_T is the transpiration rate and was measured by the eddy covariance technique, and m is canopy foliage water content and was set to the measured value of 47.8 mol m^{-2} (see section below). The molar ratios are converted to their respective counterparts in the delta notation, such as

$$\delta_L = (R_L/R_{\text{VSMOW}} - 1) \times 1000, \quad \text{‰}$$

where R_{VSMOW} is the VSMOW standard molar ratio. The inflow boundary condition is specified by δ_S. To eliminate from equation (1) $\delta_{L,e}$, which is not an observable variable, we adopted the uniform pool assumption so that $\delta_{L,e} = \delta_L$.

[9] Equation (2) was integrated at 5-min time steps. An initial value of 4‰ was assigned to δ_L before the start of the

integration. The solution became insensitive to the initial value, usually after 4 hours of integration time.

3. Experimental Methods

3.1. Site

[10] The experiment was conducted in a mixed forest in Connecticut from May to early November 2005. Details of the site information are given by *Lee and Hu* [2002]. The dominant overstory tree species were red maple (*Acer rubrum*), eastern white pine (*Pinus strobus*), beech (*Fagus grandifolia*), and hemlock (*Tsuga canadensis*). Mean tree height was 16–18 m. The dominant understory species were mountain laurel (*Kalmia latifolia*) and hayscented fern (*Dennstaedtia punctiloba*). The soil was a Holllis series spodosol, common around this part of New England. The average annual temperature was 7.0°C. The average total annual precipitation was 133 cm.

3.2. In Situ Measurement of Water Vapor and Flux Isotope Ratios

[11] The in situ system for measuring water vapor isotope ratio consisted of a tunable diode laser analyzer (TDL, model TGA-100A, Campbell Sci. Inc., Logan, Utah) and a dripper calibration device. The principle of operation was described by *Lee et al.* [2005]. In this study, several features were added to the original design to enhance its flux isotope ratio performance. As in the earlier design, vapor calibration standards were produced by the dripper, which delivered liquid water of a known isotope content (−15.8‰) at a desired rate into an evaporating flask. Because vaporization occurred instantly inside the flask, the isotope ratio of the moist air generated by the dripper was identical to that of the liquid water feed. In this study, the dripper moist air was split into two span calibration streams, and was controlled all the time to track the ambient humidity so that the mixing ratio of one span was 5% higher and the other 5% lower than the ambient humidity. The dynamic calibration procedure was needed to remove instrument nonlinearity.

[12] Another enhanced feature was a gradient interface, consisting of two 1-L buffer bottles and a series of electrical valves. Air was drawn from two heights (21.7 and 30.7 m above the ground or roughly 3 and 12 m above the treetops) though 50-m-long tubing (model Synflex 1300, 0.635 cm OD, Saint-Gobain Performance Plastics, Wayne, New Jersey), at a rate of 13 L min^{-1} STP (standard temperature and pressure) to the interface. A small portion (0.22 L min^{-1} STP) of the air sample was drawn into the buffer bottles to damp turbulent fluctuations before being analyzed by the TDL. The interface removed the TDL manifold inlet bias by alternatively switching between the two air intakes in every calibration cycle. To minimize condensation on tube walls and memory effects, the whole sampling stream, including the TDL manifold, its sample cell, the gradient interface, and the sampling tubes, was heated to temperatures greater than 40°C.

[13] The ambient vapor $^{18}O/^{16}O$ isotope ratio was calibrated in every manifold switching cycle (120 s long) using the spans produced by the dripper and a zero gas (ultra high purity nitrogen). We first applied the procedure of *Lee et al.* [2005] using the zero gas and one of the two spans and then interpolated between the two span concentrations. The interpolation further reduced the nonlinearity error in δ_V. A typical precision (one standard deviation) of hourly mean δ_V was 0.1 to 0.2‰.

[14] In situ calibration of the flux isotope ratio measurement was made hourly according to

$$R_{\mathrm{ET}} = R_d \times \frac{x_2^{16} - x_1^{16}}{x_2^{18} - x_1^{18}} \times \frac{x_3^{18} - x_4^{18}}{x_3^{16} - x_4^{16}}, \tag{3}$$

where R_{ET} is the ratio of the $H_2\,^{18}O$ molar flux to the $H_2\,^{16}O$ molar flux, or isotopic signature of the ecosystem evapotranspiration (ET), R_d is the $^{18}O/^{16}O$ molar ratio of the dripper water feed, superscripts 16 and 18 denote the ^{16}O and ^{18}O molecules, respectively, subscripts 1–4 denote TDL inlet assignments (1 and 2: span calibrations; 3 and 4: ambient air from measurement heights of 21.7 and 30.7 m), and x_i denotes TDL output (uncalibrated mixing ratio) for inlet i. The molar flux ratio was converted to the delta notation in reference to the VSMOW standard, as

$$\delta_{\mathrm{ET}} = (R_{\mathrm{ET}}/R_{\mathrm{VSMOW}} - 1) \times 1000 \quad ‰. \tag{4}$$

[15] In the derivation of equation (3), we have used the fact that the two vapor spans had isotope ratios identical to R_d and the assumption that the eddy diffusivities in ambient air are the same for water vapor molecules with different isotopes [*Griffis et al.*, 2005]. This is a valid assumption since the source distributions of these two isotopes are nearly identical in a forest [*Raupach*, 1989]. The water vapor at the sampling heights was a mixture of contributions by evapotranspiration, lateral advection, and entrainment of the free atmosphere into the boundary layer. However, because the sampling took place in the surface layer over an extensive forest, the vapor mixing ratio gradient was driven totally by the surface ET flux. For example, in a large eddy simulation of a dual-source diffusion problem, *Wyngaard and Brost* [1984] showed that the contribution of the top-down entrainment flux to the mixing ratio gradient in the surface layer is negligible.

[16] Prior to field implementation, a series of laboratory tests were made to characterize the precision of the flux isotope ratio measurement, optimize the manifold switching sequence, and determine the best construction material for the gradient interface. The most important test, which is described here, simulated the flux-gradient measurement in the field. In the test, one air inlet was fed with 100% room air. The other inlet was fed with 96% room air and 4% moist air generated by a dew-point generator. This arrangement produced a "gradient" between the two inlets of 0.3–0.5 mmol mol^{-1} in the vapor mixing ratio and 0.1–0.3‰ in the vapor isotope ratio. The magnitudes of these gradients were similar to those observed over the forest in the daytime. In the test, the dew-point generator served as a Rayleigh distillation device. The isotope ratio of its moist air followed the Rayleigh distillation prediction. The goal of the test was to determine how well the TDL measurement system could recover the known dew-point generator signal (the "flux" signal) from the gradient measurement. The

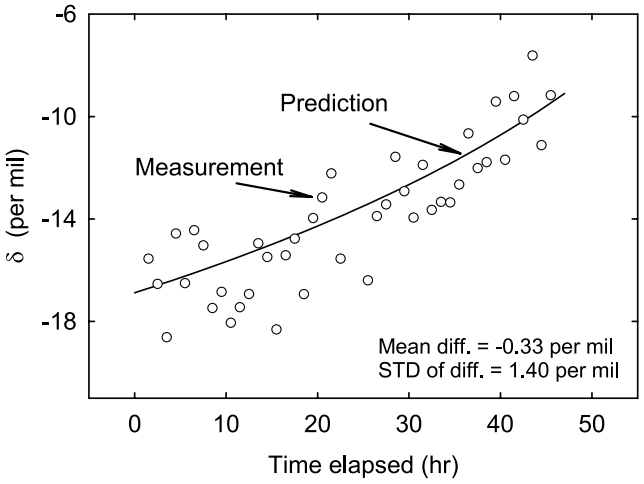

Figure 1. Results of a laboratory test that simulated the gradient-diffusion measurement in the field. Circles denote $^{18}O/^{16}O$ ratio in delta notation of the dewpoint generator vapor measured with the gradient-diffusion technique; solid line denotes prediction from the Rayleigh distillation theory.

isotope content of the dew-point generator air was computed from the TDL measurements according to equation (3) with a slight modification to account for the mixing fraction of the dew-point generator air sampled by the second inlet. The TDL measurement was compared with the prediction from the Rayleigh distillation theory as described by *Lee et al.* [2005]. The test yielded a flux isotope ratio precision of 1.4‰ (1 standard deviation) and a bias of -0.33‰ (Figure 1). We consider this as the typical measurement precision for daytime observations. The bias between the measurement and the prediction was within the uncertainty range of such comparisons [*Lee et al.*, 2005]. At night, the measurement was considerably noisier because the vertical vapor concentration gradient was much smaller than in daylight hours.

[17] The TDL measurement started on DOY (day of the year) 134 (14 May) and ended on 309 (5 November), 2005. Except for a one-week-long pump failure (DOY 260–266, 17–23 September), the observations were continuous.

3.3. Isotopic Analysis of Ecosystem Water Pools

[18] Conventional isotopic measurement was made to characterize various ecosystem water pools. Precipitation water was collected on an event basis at the site [*Welp et al.*, 2006]. Stream water was sampled weekly from a stream near the eddy flux footprint. Stem samples were collected biweekly from nongreen twigs at the midcanopy height of six overstory trees, with DBH ranging from 0.06 to 0.42 m. Soil samples were collected from the O horizon (0–5 cm depth) at three locations once every 3–7 days. Water in the stem and soil samples was extracted via cryogenic vacuum distillation. Isotopic analysis of all liquid water samples was performed in triplicate by the CO_2 equilibration technique. The equilibrated CO_2 was analyzed by continuous flow using a Europa Scientific ANCA-G and Hydra 20-20 IRMS. The sample was measured against three reference standards traceable to the primary reference standards VSMOW and SLAP distributed by the IAEA, Vienna. A typical measurement precision (one standard deviation of the triplicate analysis) was 0.05‰.

3.4. Eddy Covariance and Micrometeorological Measurement

[19] Micrometeorological variables were measured to aid the interpretation of the TDL data. The whole-ecosystem fluxes of water vapor, sensible heat, carbon dioxide and momentum were measured with the eddy covariance method [*Lee and Hu*, 2002]. The eddy covariance time series, sampled at 10 Hz, were processed to produce half-hourly flux values. Soil evaporation was measured daily with 5 homemade lysimeters between DOY 140 and 164. Soil moisture was measured once a week with a profile probe (model PR1/4, Dynamax Inc., Houston, Texas) down to a depth of 30–40 cm at six locations within the flux footprint. Other micrometeorological measurements included wind speed and direction, relative humidity, precipitation, solar radiation and net radiation.

[20] Leaf water content was measured on two days (19 July and 1 August) with leaf samples collected at the midcanopy height from the dominant tree and understory species. The measurement was scaled by species composition within the eddy flux footprint to give a canopy foliage water content of 47.8 mol m^{-2} (moles per unit ground area).

4. Results

4.1. Water Vapor Isotope Ratio

[21] Figure 2 plots all hourly observations of δ_V against the water vapor mixing ratio (w). The data can be represented by the regression equation

$$\delta_V = -40.86 + 8.36 \ln(w)$$

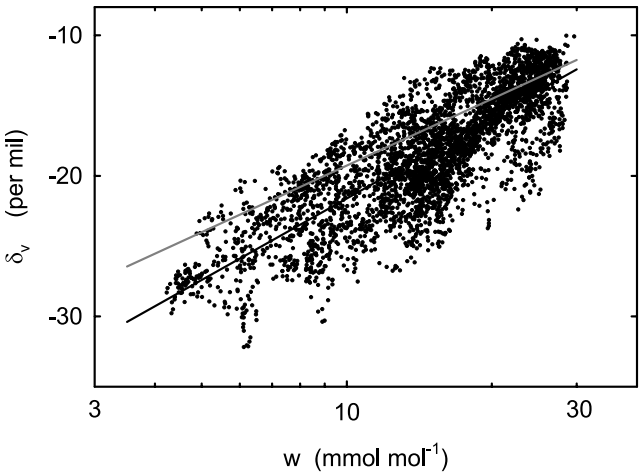

Figure 2. A log-linear plot of hourly vapor $^{18}O/^{16}O$ isotope signal δ_V versus water vapor mixing ratio w of all data collected during the field experiment at the height of 21.7 m. The black solid line represents a linear regression of the data ($\delta_V = -40.86 + 8.36 \ln(w)$, $R^2 = 0.68$, $p < 0.001$). The grey line represents the regression equation established from a data set obtained at a coastal site [*Lee et al.*, 2006].

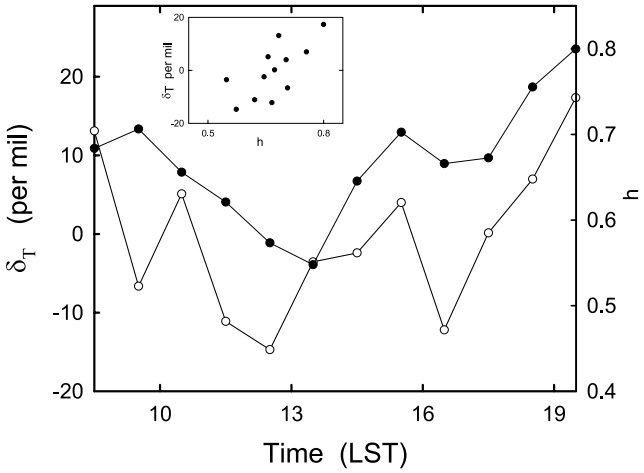

Figure 3. Correlation of the transpiration isotope value (δ_T, open circles) with relative humidity (h, solid circles) on DOY 234 (22 August). Such correlation was typical of the midday periods that experienced humidity fluctuations. Inset is a scatterplot of the same data (linear correlation = 0.69, $p < 0.05$).

[22] The log-linear dependence suggests that on a seasonal timescale, variations in δ_V were dominated by Rayleigh distillation associated with airmass life cycles. A similar log-linear relation was also observed at a coastal site in Connecticut, where for a given w, the δ_V value appeared 0.5–3.5‰ higher than the value reported here [*Lee et al.*, 2006].

[23] The hourly δ_V measured at the height of 21.7 m was slightly higher than that measured at the height of 30.7 m. The mean difference was 0.10‰ (standard deviation 0.11‰, number of observations n = 1541) for all the data obtained in rainless and dew-free conditions. The difference did not show statistically significant correlation with time of the day, relative humidity, or water vapor flux, and was comparable to the δ_V measurement precisions reported for the TDL and mass spectrometer techniques. The Keeling mixing line approach, as applied to the analysis of flask air samples, would suffer a much larger noise level for the flux isotope ratio estimation than reported here. It appears that, by computing the flux ratio according to equation (3), some of the covarying noises in the individual isotopologue measurements were canceled out, enabling us to resolve the flux ratio signal.

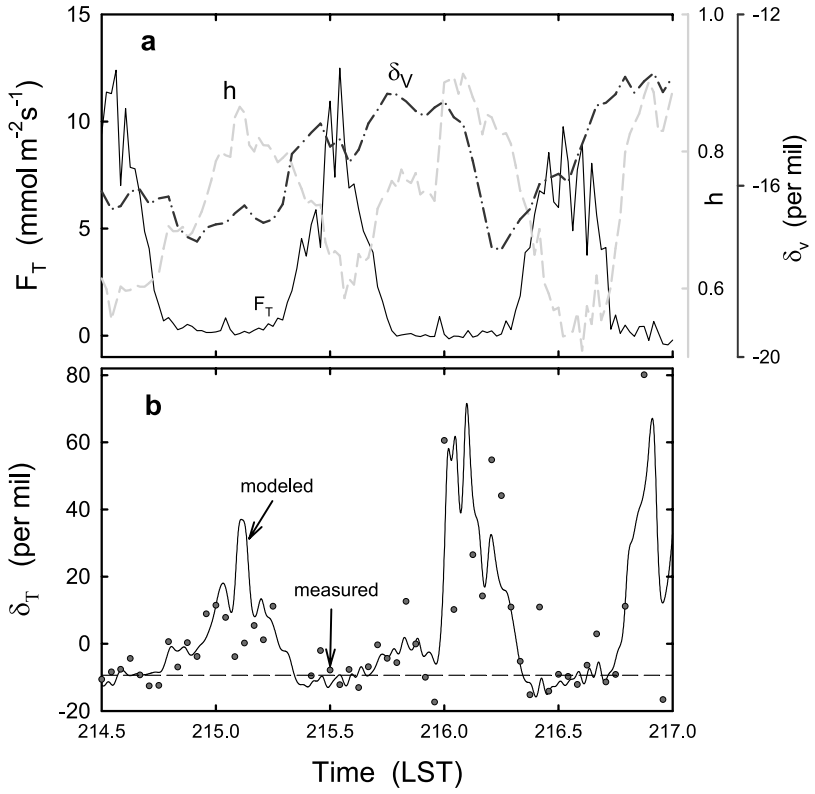

Figure 4. Diurnal variation of the transpiration $^{18}O/^{16}O$ isotope signal (δ_T), DOY 214–216 (2–4 August). (a) Three observed environmental drivers: relative humidity (h), the whole-canopy transpiration rate (F_T), and the $^{18}O/^{16}O$ ratio of water vapor (δ_V). (b) Measured (dots) and modeled (line) δ_T. The isotope value of stem water of overstory trees is −9.5‰ at this time and is indicated by the dashed line in Figure 4b.

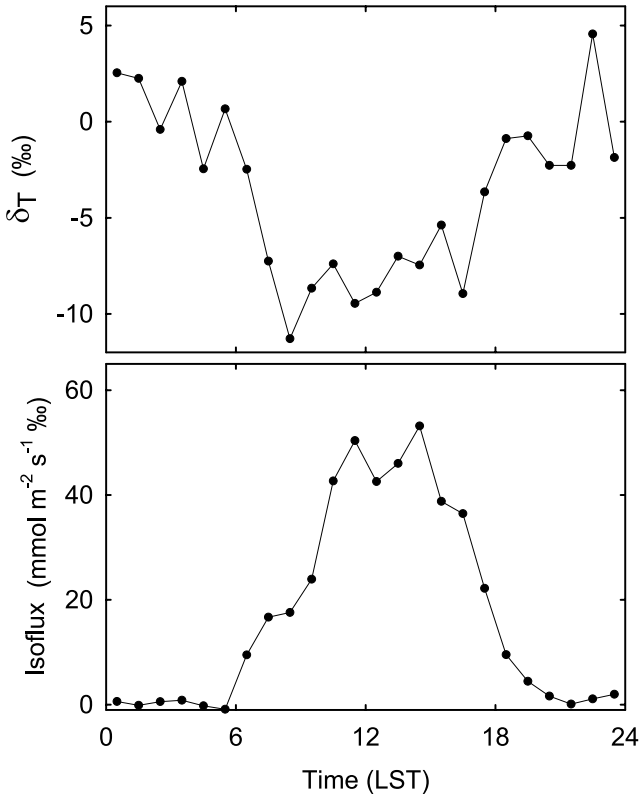

Figure 5. Ensemble mean diurnal variation of (top) the transpiration isotope ratio δ_T and (bottom) isoflux before leaf senescence. The standard deviation of the ensemble δ_T data varies from 10‰ at noon to 20‰ at midnight. Factors contributing to the standard deviation include instrument noise (Figure 1) and natural day-to-day variation (Figure 4). Measurements impacted by dew formation, rain, and evaporation of intercepted rainwater are excluded from the ensemble analysis.

4.2. Short-Term Variations in δ_T

[24] Figures 3–6 present the δ_T data on the hourly to multiday timescales. The reader should be aware of two points before interpreting these figures. First, soil evaporation, measured with the lysimeters, was negligibly small, contributing less than 5% to the total ET measured by the eddy covariance. Other researchers have also reported similarly small soil evaporation fractions in midlatitude forests [*Blanken et al.*, 2001; *Wilson et al.*, 2001]. Throughout the rest of the paper, the measured ET and δ_{ET} (equations (3) and (4)) were taken to be the same as F_T and δ_T, respectively, before leaf senescence (roughly DOY 270). Second, h in these plots and the subsequent model calculations was referenced to the saturation vapor pressure at canopy temperature T_c, which was estimated according to the aerodynamic principle, as

$$T_c = T_a + \frac{(\overline{w'T'})\,u}{u_*^2}$$

where T_a is air temperature, $\overline{w'T'}$ is kinematic sensible heat flux, u is wind speed, and u_* is friction velocity.

[25] Figures 3 and 4 show evidence of the influence of h on δ_T on the hourly to the diurnal timescales. In daylight hours, h usually displayed a U-shaped pattern, which was followed by δ_T (Figure 4). On some days, the U-shaped humidity pattern was interrupted by mesoscale weather disturbances. The influence of the associated h variations on the δ_T time series was clearly discernible. For example, the linear correlation (r) of h and δ_T was 0.69 between 8:00 and 20:00 on DOY 234 and was statistically significant (Figure 3; $n = 12$, confidence level $p < 0.05$).

[26] There was a reasonably good agreement between the observed and modeled δ_T (Figure 4). The modeled δ_T reached minimum values of −12.7 and −15.8‰ around 0900 LST on DOY 215 and 216, respectively, which were lower than the δ_S value of −9.4 measured on DOY 213, and increased slowly with time through the daylight hours. The progressive increase of the modeled δ_T in the daytime was consistent with the ensemble trend (Figure 5) and was suggested by the observed δ_T on these two days. On DOY 214, the transition to the night period was rather gradual, a pattern in accord with the measurement. On DOY 215, the modeled δ_T showed a sudden increase at 2400 LST, which was consistent with the observational evidence and must have been caused by a rapid increase in h. On DOY 216, a rapid increase in the modeled δ_T occurred around 1900 LST, at the same time when F_T was decreasing rapidly owing to stomatal closure and h was increasing owing to canopy cooling. Once again, the day-to-night transition on DOY 216 was also evident in the observation. As stated above, relative humidity was measured in reference to canopy temperature. Use of air relative humidity would cause a negligible change to the modeled result for the daylight hours, but would delay the abrupt day-to-night transition on DOY 215 and 216 by about 1 hr. On the late evening of DOY 216, both the observed and modeled δ_T showed large hour-to-hour oscillations (>60‰), suggesting that δ_T was extremely sensitive to environmental perturbations at night.

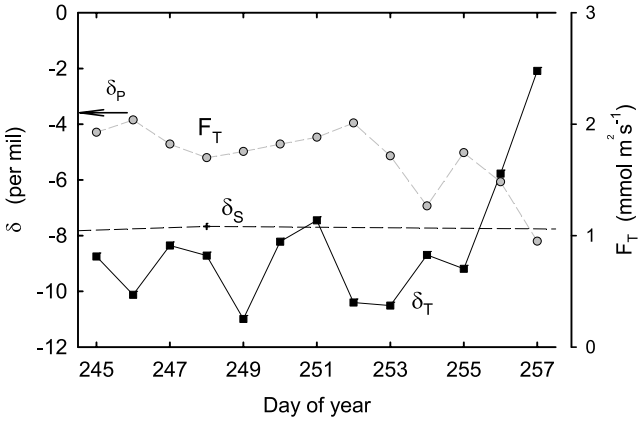

Figure 6. Multiday variation of the daytime flux-weighted δ_T (squares) and 24-hour mean transpiration rate (F_T, grey circles) over DOY 245–257 (2–14 September). The dashed line indicates the $^{18}O/^{16}O$ ratios of the stem water of overstory trees. The arrow indicates the isotope value of precipitation falling between DOY 240–243.

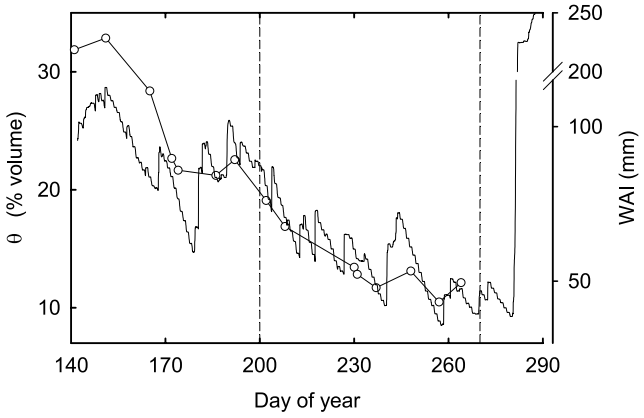

Figure 7. Seasonal variations of the 0- to 30-cm volumetric soil water content (θ, line with open circles) and water availability index (WAI, solid line).

[27] To bring out the diurnal pattern more clearly, in Figure 5 (top), we present an ensemble mean diurnal variation of δ_T computed with all valid observations over the growing season. Excluded from the ensemble analysis were periods of dew formation and data collected on days that were impacted by rain and the subsequent evaporation of foliage-intercepted rainwater. The ensemble mean displayed a minimum of −10‰ and a maximum of 5‰. The minimum value occurred at approximately 0900 LST, or 2 hr after sunrise, and coincided with the rapid decrease in h and increase in F_T. The δ_T value increased slowly with time through the daylight hours, owing to a progressive enrichment of the leaf water. A similar trend was also suggested by the model simulation of *Lai et al.* [2005] for an old growth Douglas fir forest. On individual days, the peak-to-peak diurnal change could be much larger than the ensemble mean, sometimes exceeding 60‰ (Figure 4).

[28] The δ_T time series also experienced substantial variations over periods longer than a week, as shown in Figure 6. The measurement presented here was for a 13-day period in early September, which was the longest rainless period in the 2005 growing season and hence there was no gap in the δ_T data. Here δ_T was the daytime flux-weighted value to avoid the noisy nighttime data. The observed δ_T varied in the range of −11.0 to −2.1‰, with a flux weighted mean value of −8.7‰ over the whole period. For comparison, the δ_S value, sampled on DOY 248, was −7.7‰. The isotope value of soil water in the top layer (0–5 cm depth) was −5.4 and −3.4 on DOY 246 and 253, respectively. The three rain events falling just before this period (DOY 240–243) had an amount-weighted average isotope value of −3.7‰. On at least 10 days in this period, the daytime transpiration isotope ratio was systematically lower than that of the source water. Unlike the subday variations (Figure 2), h was not a good predictor of the daytime flux-weighted δ_T (r = 0.23, n = 13). Instead, the flux-weighted δ_T was found to correlate significantly with F_T (r = −0.74, n = 13, $p < 0.01$).

[29] The ensemble mean isoflux is shown in Figure 5 (bottom). The isoflux, computed as $(\delta_T - \delta_V)F_T$, was positive for every hour of the day. In other words, transpiration always acted to enrich the surface and boundary layer air with ^{18}O. The time rate of change of δ_V can be assessed with the rate equation

$$\frac{d\delta_V}{dt} = \frac{1}{M}(\delta_T - \delta_V)F_T,$$

where M is the column molar number of water vapor in the atmospheric boundary layer over a unit ground area. Given an average isoflux value of 17 mmol $m^{-2}s^{-1}$ per mil and a typical value of 1000 mol m^{-2} for M, the rate of increase was on the order of 1.5‰ over a 24-hour period. However, this transpiration effect was easily masked by other confounding factors, such as airmass advection, entrainment of air in the free atmosphere into the boundary layer [*Lee et al.*, 2006], and mixing of the boundary layer air with the canopy air [*Lai et al.*, 2005].

4.3. Seasonal Variations in Soil Water Content and δ_S

[30] Figure 7 presents the volumetric soil water content (θ) and water availability index (WAI) over the course of the experimental period. Here θ was for the 0- to 30-cm soil layer and was averaged over the six measurement locations. WAI at time t was computed according to the water balance equation, as

$$\mathrm{WAI} = \theta_o + \int_0^t (P - \mathrm{ET})dt$$

where θ_o is the initial water content in the 0- to 30-cm soil layer and P is precipitation. The experiment could be divided into three periods. The transition from the first to the second period occurred around DOY 200 (19 July). Prior to DOY 200, some fluctuations in WAI were evident, but in general precipitation was able to meet the evapotranspiration demand. After DOY 200, P was exceeded by ET, resulting in a rapid decline in WAI in the top soil layer where over 70% of the root biomass resided. During the second period (DOY 200–270), the average soil moisture in the 0- to 30-cm soil layer was reduced to 14% (by volume) from 26%, the average value for the first period. During leaf senescence (DOY 271–309), the declining trend in WAI was reversed in response to a long period of rainy weather and a reduced ET demand.

[31] The seasonal course of δ_S is shown in Figure 8, along with the isotopic ratios of ET and precipitation. A feature notable of the seasonal data was the remarkably slow change in δ_S, from −10.0‰ in June increasing progressively to −7.7‰ in September, despite large temporal variability in the precipitation isotope ratio. Variations of δ_S among the six trees sampled were relatively small. The δ_S standard deviation was 0.9‰ in early June, stabilized at 0.5‰ over most part of the growing season, and increased to the highest value of 1.7‰ in early October during leaf senescence. The correlation of the seasonal mean δ_S with DBH was not statistically significant (r = 0.26, n = 6). Isotopically, the overstory trees appeared to function as one entity despite variations in tree size and surface soil moisture.

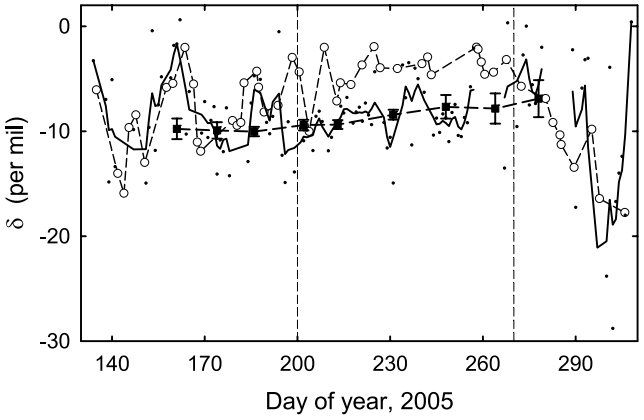

Figure 8. Seasonal variations of isotope ratios of ET (dots, δ_{ET}), precipitation (circles, δ_P), and stem water (squares, δ_S). Also shown is a 5-day running average of δ_{ET} (solid line). Error bars indicate 1 standard deviation.

4.4. Seasonal Variation in δ_{ET}

[32] On the seasonal timescale, the behavior of δ_{ET} was complex (Figure 8). Once again, δ_{ET} was presented as the daytime (0800–1900 LST) mean value weighted by water vapor flux. The time series can be roughly divided into three periods. Here δ_{ET} was regarded as being equivalent to δ_T in the first and second period but not in the third, as noted below.

4.4.1. Early Growing Season (Before DOY 200)

[33] δ_{ET} was closely coupled with changes in δ_P. A rain event with an unseasonably low isotope value (−15.9‰) occurred on 144, reducing δ_{ET} to a similar level. This was followed by an increasing trend from DOY 150 to 164, a decreasing trend from DOY 165 to 179, and a second increasing trend from DOY 180 to 188, in both δ_{ET} and δ_P.

4.4.2. Late Growing Season (DOY 200–270)

[34] The day-to-day variation of δ_{ET} was decoupled from δ_P and instead was centered around δ_S of the overstory trees. Over this period, δ_{ET} was negatively correlated with the ET rate (r = -046., n = 46, $p < 0.01$; see also Figure 6).

4.4.3. Leaf Senescence Transition (DOY 271–309)

[35] As pointed out earlier, δ_{ET} was taken to be the same as δ_T during the growing season because of the negligibly small contribution of soil evaporation to ET. This approximation was not valid in leaf senescence because soil and litter evaporation became important owing to the opening up of the canopy and the excessive soil moisture (Figure 7). This may explain why δ_{ET} was considerably more variable than before. Despite the noise, the data seem to indicate a rapid decrease with time in the flux isotope ratio that coincided with the decreasing trend in δ_P, and an increase with time which may be related to the evaporative enrichment of water in the fresh litter layer.

4.5. Isotopic Ratio of Ecosystem Water Pools and Fluxes

[36] Figure 9 summarizes the $^{18}O/^{16}O$ isotopic signal of various ecosystem water pools and fluxes before leaf senescence. The analysis was restricted to fair weather periods. Evaporation of the intercepted rain and stream water discharge during and immediately after storm events were not considered. The isotope ratios of precipitation and ET were the mean values weighted by precipitation amount and water vapor flux, respectively. The isotope ratios of surface soil, streamflow and water vapor were the algebraic mean values of all the valid observations. The $^{18}O/^{16}O$ isotopic ratios of water in the shallow and deep soil were assumed to be the same as the summer rain and stem water

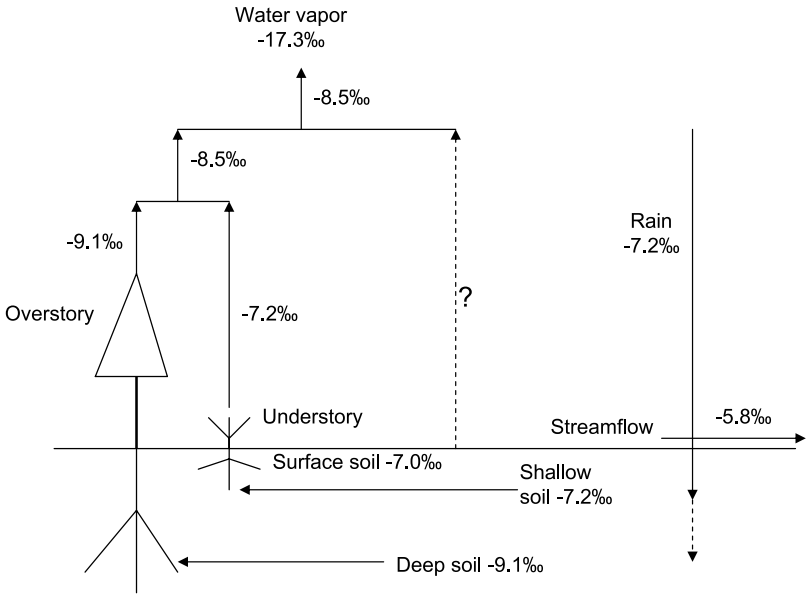

Figure 9. A schematic representation of the $^{18}O/^{16}O$ isotopic value of various ecosystem pools and fluxes.

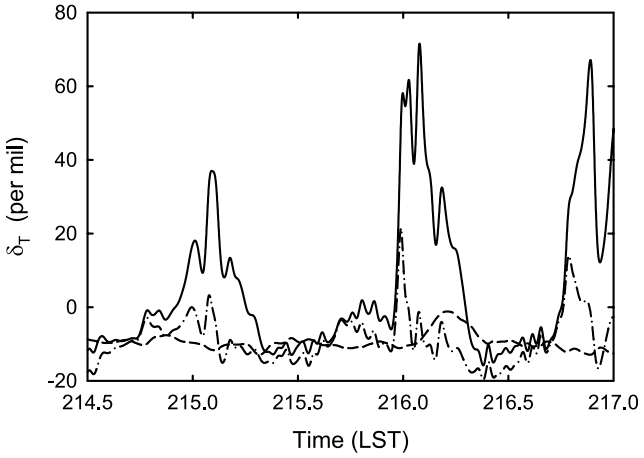

Figure 10. Model sensitivity analysis for DOY 214–216 (2–4 August): Dash-dotted line, the transpiration rate F_T was held constant (at 2.4 mmol $m^{-2}s^{-1}$, the mean over this period) and relative humidity h varied according to the observations (Figure 4a); dashed line, h was held constant (at 0.77) and F_T varied according to the observations; and solid line, both F_T and h varied according to the observations.

of the overstory trees, respectively (section 5.3). The influence of soil evaporation on δ_{ET} was ignored. This last approximation was justified by isotopic evidence: the isotopic value of water in the surface soil (0–5 cm depth) was only 0.2‰ higher than δ_P.

5. Discussion

5.1. Influences of h and F_T on δ_T

[37] The data in Figure 3, and to a lesser extent in Figure 4, show that on timescales of a few hours, h was an important driver of the δ_T variations. Indeed, the positive correlation shown in Figure 3 was typical of many other midday periods that had experienced h fluctuations. To explain this correlation, we can rearrange equation (1), using the approximations $\alpha_{eq} \simeq 1$ and $\epsilon_k/1000 \ll 1$, to isolate the humidity effect. We obtain

$$\delta_T \simeq \frac{\delta_L - \delta_V - \epsilon_{eq}}{1-h} + \delta_V - \epsilon_k. \quad (5)$$

Let us now compare the magnitude of the three quantities in the numerator of the first term of equation (5). The equilibrium fractionation factor ϵ_{eq} was a weak function of temperature, varying in a narrow range of 9.3 to 10.6‰ during the growing season. The mean δ_V over the growing season was −17.3‰, with hourly values never exceeding −10‰ (Figure 2; the highest values were observed during rain events). Although no measurement was made of δ_L, numerical calculations based on equations (1) and (2) suggest that it varied diurnally, with a minimum of 0.1‰ (ensemble mean over the growing season) occurring at 08:00 LST and a maximum of 4.5‰ at 16:00 LST. This is consistent with the published evidence showing that δ_L is generally positive in daylight hours [e.g., *Cernusak et al.*, 2005]. Model calculations of *Farquhar et al.* [1993] give an estimate of a global mean δ_L of 4.4‰. Thus the numerator of the first term of equation (5) should be positive. According to equation (5), δ_T will adjust instantly to perturbations in h, and if other factors are approximately constant, the $\delta_T - h$ correlation should be positive although not strictly linear. A positive correlation is also suggested by the observation of *Harwood et al.* [1999].

[38] We stress that the $\delta_T - h$ correlation is robust only on timescales of a few hours in the daytime. On longer timescales, the temporal dynamics of F_T have a large effect on leaf water turnover and hence δ_L. To investigate the role of F_T, we present in Figure 10 the result of a model sensitivity analysis. When F_T was held constant, the simulated δ_T showed high-frequency fluctuations driven by the observed fluctuations in h. In contrast, when h was held constant, the simulated δ_T time series was very smooth, suggesting insensitivity to the short-term fluctuations in F_T. Only by covarying both h and T according to the observations (Figure 4a) was the model able to reproduce the observed large diurnal variation in δ_T (Figure 4b and Figure 10). Indeed, a low F_T coupled with high h after a period of high F_T appeared necessary to produce a large δ_T. This is because at times of low F_T, little dilution would occur to the δ_L signal enriched in the preceding period of high F_T, and a high h served to amplify the signal as the denominator of the first term in equation (5) became very small. Hence the diurnal variation in δ_T was a transient phenomenon resulting from the variable canopy microclimate on the diurnal timescale.

[39] We suggest that the $\delta_T - F_T$ correlation on the multiday timescale (Figure 6) was also a transient phenomenon. On a day of reduced F_T, the dilution of ^{18}O in the foliage water was slow owing to the long isotopic turnover time. For example, DOY 257 experienced a reduced transpiration rate; the turnover time τ was about 5 hr according to $\tau = m\,(1-h)/F_T$ [*Farquhar and Cernusak*, 2005]. Additionally, a low daytime F_T was usually associated with cloudy skies when h was high, which again would amplify the effect of δ_L on δ_T (equation (5)).

5.2. Steady State Assumption

[40] Measurement of δ_T provides the most direct test of the steady state assumption (SSA). Laboratory investigations show that δ_T will respond to a step change in h [*Wang and Yakir*, 1995], δ_V [*Roden and Ehleringer*, 1999], and δ_S [*Roden and Ehleringer*, 1999; *Dongmann et al.*, 1974]. *Wang and Yakir* [1995] simulated experimentally the effect of covariations of h and F_T. They found that δ_T is 3‰ lower than δ_S at "midday" and approximately equals the latter at "night." Their diurnal variation is smaller than the range reported here because in their laboratory simulation, the transpiration rate changes by less than twofold whereas in the field conditions, the nighttime transpiration rate was an order of magnitude smaller than the midday value (Figure 4a). Using a gas exchange chamber, *Harwood et al.* [1998] found that δ_T is lower in the morning and higher in the afternoon compared with δ_S under field conditions on two days, with a total change of 25‰.

[41] Our study is in broad agreement with the leaf and plant-scale studies cited above. It adds to a growing body of evidence showing that the SSA is, in general, not satisfied in the field where canopy microclimatic conditions are highly variable. At the canopy scale, the departure from the steady state was most evident at night (Figure 4) and on days of low F_T (Figure 6). While the nonsteady state behavior was not a surprise, the large departure from steady state at night (>60‰, Figure 4b) was not expected.

5.3. Temporal Dynamics of Forest Water Use

[42] To examine the temporal dynamics of forest water use, we propose that the soil water could be separated into two pools, a shallow pool that was repeatedly recharged by summer rain and a deep stable pool that represented a mixture of winter precipitation and a portion of the summer rain that had infiltrated downward (Figure 9). The understory plants were able to access only the shallow pool because of their shallow roots. The overstory trees could draw water from both pools, although the fact that their δ_S value was insensitive to individual rain events suggests that they relied almost exclusively on the deep pool (Figure 8). Over the growing season, the mean δ_S and δ_P were -9.1, and -7.2‰, respectively. The mean δ_T, weighted by the eddy covariance water vapor flux, was -8.5‰ over the growing season, a value that was very close to δ_S and was indicative of a large contribution of the overstory trees to the whole-canopy transpiration.

[43] The small temporal variation in δ_S (Figure 8) was consistent with the study of *Brandes et al.* [2007] but was in contrast to the study of *White et al.* [1985] who have documented a 40‰ change in the D/H ratio of xylem sap in eastern white pine over a 5-day period following a summer rain event. In a four-site comparative study in Oregon, δ_S shows progressive increase through time at two of the sites but not at the other sites [*Bowling et al.*, 2003].

[44] The fractional contribution of the overstory trees to the whole-canopy transpiration can be estimated from the isotopic data, as

$$f = \frac{\delta_T - \delta_P}{\delta_S - \delta_P}. \quad (6)$$

Equation (6) assumes that the $^{18}O/^{16}O$ isotopic ratio of the understory transpiration can be approximated by the rain value as discussed above. Substituting the observed values in equation (6), we obtained an estimate of $f = 0.70$. By comparing sap flow and eddy covariance measurements, *Granier et al.* [2000] estimated that the ratio of the overstory transpiration to the total stand transpiration is 0.77 for two beech forests in France. *Blanken et al.* [2001] compared the eddy flux over and below the overstory canopy of an even aged aspen forest using two eddy covariance systems. They reported a ratio of 0.71. In a study that compares methods of measuring forest evapotranspiration in a mixed species temperate forest, *Wilson et al.* [2001] found that the overstory transpiration is only 50% of the total transpiration flux. The authors attribute the low value partly to the inaccuracy in scaling up the sap flow data to the whole stand. In our case, it would extremely difficult to apply the sap flow method owing to species diversity and spatial variability in soil moisture. Similarly, it was impractical to deploy the dual eddy covariance method because there was no open trunk space that separated the overstory and understory canopy layers.

[45] Of course, flux partitioning using isotope labeling was not without its own limitations. Given the large day-to-day variations in δ_T, flux partitioning was difficult at the daily or even weekly timescale (Figure 8). These variations were caused in part by the lack of good nighttime data and the nonsteady state behavior of δ_T. In cases where the data on δ_T are limited to a short duration (e.g., a few hours), recovery of the true source signal will likely require parameter estimation methods that utilize a validated model for the ecosystem-scale isotopic exchange.

[46] A close inspection of the three time series, δ_{ET}, δ_P and δ_S, allows us to further understand the dynamics of the component transpiration fluxes (Figure 8). Once again, the reader is reminded that δ_{ET} was regarded as being equivalent to δ_T before leaf senescence. In the early growing season, the δ_{ET} and δ_P values were tightly coupled, indicating that the understory plants must have played a large part in the whole-canopy transpiration at this time. Partitioning with equation (6) was however difficult because the two end members δ_P and δ_S had similar values (-9.1 and -9.8‰, respectively). The δ_{ET} time series showed a transition around DOY 200 corresponding to the rapid drying of the 0- to 30-cm soil layer (Figure 7). After DOY 200, δ_{ET} was decoupled from δ_P and instead fluctuated around δ_S. Thus the overstory trees dominated the whole-stand transpiration. Or from an ecosystem-scale viewpoint, instead of drawing water from the shallow pool, the forest switched its water use strategy to rely almost exclusively on the deep pool in the late growing season. During this period, the contribution to the whole-canopy transpiration from the understory plants, if any, appeared to be too small to be discernible within the uncertainty of the δ_{ET} measurement.

[47] Temporal shifts in water use have been extensively studied at the plant scale using water isotope labeling [*Dawson et al.*, 1998]. These shifts are usually associated with the onset of the dry period in environments where wet and dry seasons are present. As the top soil dries out, woody plants become more dependent on deep soil water and groundwater for transpiration [*Zencich et al.*, 2002; *Ewe and Sternberg*, 2002; *Williams and Ehleringer*, 2004; *Smith et al.*, 1997; *Thorburn et al.*, 1993]. Figure 8 demonstrates that the phenomena could also occur at the ecosystem scale and in the semihumid southern New England climate where precipitation was evenly distributed throughout the year. In our case, depletion of water in the shallow pool was not caused by a lack of rain input, but rather by ET exceeding precipitation in the late growing season (Figure 7). The rapid shift to the deep water pool around DOY 200 can be considered an example of switches in biophysical regulations of ecosystem processes [*Baldocchi et al.*, 2006].

5.4. Modeling the Ecosystem Isotopic Exchange of Water Vapor

[48] Theoretical models play an indispensable role in the investigation of isotopic exchange between plants and the

atmosphere. The model deployed in this study was an application of the Dongmann model at the canopy scale. It was kept deliberately in its simple form, free of tunable parameters, so that its solution could be achieved numerically using the observed variables (h, F_T, δ_V, δ_S) as inputs. In doing so, it was assumed that the foliage water pool was uniformly enriched to a single δ value and that temporal variation of the leaf water content was negligible. Despite the simplicity, the model seemed to reproduce reasonably well the broad features of the observed δ_T (Figure 4). The model calculations suggest the important role of covarying h and F_T in the nonsteady state behavior of the vapor isotopic exchange.

[49] Although not the focus of this study, improvements to the model can be made on several fronts. Future model refinement should consider ways to handle the temporal variability in the leaf water content [*Yakir*, 1998]. It is also desirable to stratify the canopy foliage water into at least two pools, with one being supplied by plants with shallow roots and sensitive to individual rain events and the other by plants with deep roots that can tap into the deep soil pool and groundwater and hence more stable with time (Figures 8 and 9). These pools are configured in parallel, not connected in series. The latter configuration is shown to be the appropriate one for modeling the so-called ''chain of lakes'' effects on the progressive evaporative enrichment along veins of a leaf [*Helliker and Ehleringer*, 2000]. Evidence of a two-layer soil water compartmentation is also given by *Jackson et al.* [1999], *Dodd et al.* [1998] and *Flanagan et al.* [1992].

[50] **Acknowledgments.** This work was supported by the U. S. National Science Foundation through grants EAR-0229343 and DEB-0514904. We thank the Great Mountain Forest Corporation, Connecticut for its in-kind contribution that supports the field facility at the Great Mountain site, and we thank the two anonymous journal reviewers for their constructive criticisms.

References

Baldocchi, D., J. Tang, and L. Xu (2006), How switches and lags in biophysical regulators affect spatial-temporal variation of soil respiration in an oak-grass savanna, *J. Geophys. Res.*, *111*, G02008, doi:10.1029/2005JG000063.

Blanken, P., T. A. Black, H. H. Neumann, G. den Hartog, P. C. Yang, Z. Nesic, and X. Lee (2001), The seasonal water and energy exchange above and within a boreal aspen forest, *J. Hydrol.*, *245*, 118–136.

Bowling, D. R., N. G. McDowell, J. M. Welker, B. J. Bond, B. E. Law, and J. R. Ehleringer (2003), Oxygen isotope content of CO_2 in nocturnal ecosystem respiration: 1. Observations in forests along a precipitation transect in Oregon, USA, *Global Biogeochem. Cycles*, *17*(4), 1120, doi:10.1029/2003GB002081.

Brandes, E., et al. (2007), Assessing environmental and physiological controls over water relations in a Scots pine stand through analyses of stable isotope composition of water and organic matter, *Plant Cell Environ.*, *30*, 113–127.

Cernusak, L. A., G. D. Farquhar, S. C. Wong, and H. Stuard-Williams (2004), Measurement and interpretation of the oxygen isotope composition of carbon dioxide respired by leaves in the dark, *Plant Physiol.*, *136*, 3350–3363.

Cernusak, L. A., G. D. Farquhar, and J. S. Pate (2005), Environmental and physiological controls over oxygen and carbon isotope composition of Tasmanian blue gum, *Eucalyptus globulus, Tree Physiol.*, *25*, 129–146.

Dawson, T. E., R. C. Pausch, and H. M. Parker (1998), The role of hydrogen and oxygen stable isotopes in understanding water movement along the soil-plant-atmospheric continuum, in *Stable Isotopes: Integration of Biological, Ecological and Geochemical Processes*, edited by H. Griffiths, pp. 169–183, BIOS Sci., Oxford, U.K.

Dodd, M. B., W. K. Lauenroth, and J. M. Welker (1998), Differential water resource use by herbaceous and woody plant life-forms in a shortgrass steppe community, *Oecologia*, *117*, 504–512.

Dongmann, G., H. W. Nünberg, H. Föstel, and K. Wagener (1974), On the enrichment of $H_2{}^{18}O$ in the leaves of transpiring plants, *Radiat. Environ. Biophys.*, *11*, 41–52.

Ewe, S. M. L., and L. S. L. Sternberg (2002), Seasonal water-use by the invasive exotic, Schinus terebinthifolius, in native and disturbed communities, *Oecologia*, *133*, 441–448.

Farquhar, G. D., and L. A. Cernusak (2005), On the isotopic composition of leaf water in the non-steady state, *Funct. Plant Biol.*, *32*, 293–303.

Farquhar, G. D., J. Lloyd, J. A. Taylor, L. B. Flanagan, J. P. Syvertsen, K. T. Hubick, S. C. Wong, and J. R. Ehleringer (1993), Vegetation effects on the isotope composition of oxygen in atmospheric CO_2, *Nature*, *363*, 439–443.

Flanagan, L. B., J. P. Comstock, and J. R. Ehleringer (1991), Comparison of modeled and observed environmental influences on the stable oxygen and hydrogen isotope composition of leaf water in *Phaseolus vulgaris* L, *Plant Physiol.*, *96*, 588–596.

Flanagan, L. B., J. R. Ehleringer, and J. D. Marshall (1992), Differential uptake of summer precipitation among co-occurring trees and shrubs in a pinyon-juniper woodland, *Plant Cell Environ.*, *15*, 831–836.

Granier, A., P. Biron, and D. Lemoine (2000), Water balance, transpiration and canopy conductance in two beech stands, *Agric. For. Meteorol.*, *100*, 291–308.

Griffis, T. J., X. Lee, J. M. Baker, S. D. Sargent, and J. Y. King (2005), Feasibility of quantifying ecosystem-atmosphere $C^{18}O^{16}O$ exchange using laser spectroscopy and the flux-gradient method, *Agric. For. Meteorol.*, *135*, 44–60.

Harwood, K. G., J. S. Gillon, H. Griffiths, and M. S. J. Broadmeadow (1998), Diurnal variation of $\delta^{13}CO_2$, $\Delta C^{18}O^{16}O$ and evaporative site enrichment of $\delta H_2{}^{18}O$ in *Piper aduncum* under field conditions in Trinidad, *Plant Cell Environ.*, *21*, 269–283.

Harwood, K. G., J. S. Gillon, A. Roberts, and H. Griffiths (1999), Determinants of isotopic coupling of CO_2 and water vapour within a *Quercus petraea* forest canopy, *Oecologia*, *119*, 109–119.

He, H., X. Lee, and R. B. Smith (2001), Deuterium in water vapor evaporated from a coastal salt marsh, *J. Geophys. Res.*, *106*, 12,183–12,191.

Helliker, B. R., and J. R. Ehleringer (2000), Establishing a grassland signature in veins: ^{18}O in the leaf water of C_3 and C_4 grasses, *Proc. Natl. Acad. Sci.*, *97*, 7894–7898.

Hoffmann, G., et al. (2004), A model of the Earth's Dole effect, *Global Biogeochem. Cycles*, *18*, GB1008, doi:10.1029/2003GB002059.

Jackson, P. C., et al. (1999), Partitioning of soil water among tree species in a Brazilian Cerrado ecosystem, *Tree Physiol.*, *19*, 717–724.

Lai, C. T., J. R. Ehleringer, B. J. Bond, and K. T. Paw U (2005), Contributions of evaporation, isotopic non-steady state transpiration, and atmospheric mixing on the $\delta^{18}O$ of water vapor in Pacific Northwest coniferous forests, *Plant Cell Environ.*, *29*, 77–94.

Lee, X., and X. Hu (2002), Forest-air fluxes of carbon and energy over non-flat terrain, *Boundary Layer Meteorol.*, *103*, 277–301.

Lee, X., S. Sargent, R. Smith, and B. Tanner (2005), In-situ measurement of water vapor $^{18}O/^{16}O$ isotope ratio for atmospheric and ecological applications, *J. Atmos. Oceanic Technol.*, *22*, 555–565.

Lee, X., R. Smith, and J. Williams (2006), Water vapor $^{18}O/^{16}O$ isotope ratio in surface air in New England, USA, *Tellus, Ser. B*, *58*, 293–304.

Raupach, M. R. (1989), A practical Lagrangian method for relating scalar concentrations to source distributions in vegetation canopies, *Q. J. R. Meteorol. Soc.*, *115*, 609–632.

Riley, W. J., C. J. Still, B. R. Helliker, M. Ribas-Carbo, and J. A. Berry (2003), O^{18} composition of CO_2 and H_2O ecosystem pools and fluxes in a tallgrass prairie: Simulations and comparisons to measurements, *Global Change Biol.*, *9*, 1567–1581.

Roden, J. S., and J. R. Ehleringer (1999), Observations of hydrogen and oxygen isotopes in leaf water confirm the Craig-Gordon model under wide-ranging environmental conditions, *Plant Physiol.*, *120*, 1165–1173.

Seibt, U., L. Wingate, J. A. Berry, and J. Lloyd (2006), Non-steady state effects in diurnal 18O discrimination by Picea sitchensis branches in the field, *Plant Cell Environ.*, *29*, 928–939.

Smith, D. M., P. G. Jarvis, and J. C. W. Odongo (1997), Sources of water used by trees and millet in Sahelian windbreak systems, *J. Hydrol.*, *198*, 140–153.

Sternberg, L. S. L. (1988), D/H ratios of environmental water recorded by D/H ratios of plant lipids, *Nature*, *335*, 59–61.

Thorburn, P. J., T. J. Hatton, and G. R. Walker (1993), Combining measurements of transpiration and stable isotopes of water to determine groundwater discharge from forests, *J. Hydrol.*, *150*, 563–587.

Wang, X. F., and D. Yakir (1995), Temporal and spatial variations in the oxygen-18 content of leaf water in different species, *Plant Cell Environ.*, *18*, 1377–1385.

Welp, L. R., J. T. Randerson, and H. P. Liu (2006), Seasonal exchange of CO_2 and $d^{18}O$-CO_2 varies with postfire succession in boreal forest ecosystems, *J. Geophys. Res.*, *111*, G03007, doi:10.1029/2005JG000126.

White, J. W. C., E. R. Cook, J. R. Lawrence, and W. S. Broecker (1985), The D/H ratios of sap in trees: Implications for water sources and tree ring D/H ratios, *Geochim. Cosmochim. Acta*, *49*, 237–246.

Williams, D. G., and J. R. Ehleringer (2004), Intra- and interspecific variation for summer precipitation use in pinyon-juniper woodlands, *Ecol. Monogr.*, *70*, 517–537.

Williams, D. G., et al. (2004), Evapotranspiration components determined by stable isotope, sap flow and eddy covariance techniques, *Agric. For. Meteorol.*, *125*, 241–258.

Wilson, K. B., P. J. Hanson, P. J. Mulholland, D. D. Baldocchi, and S. D. Wullschleger (2001), A comparison of methods for determining forest evapotranspiration and its components: sap-flow, soil water budget, eddy covariance and catchment water balance, *Agric. For. Meteorol.*, *106*, 153–168.

Wyngaard, J. C., and R. A. Brost (1984), Top-down and bottom-up diffusion of a scalar in the convective boundary layer, *J. Atmos. Sci.*, *41*, 102–112.

Yakir, D. (1998), Oxygen-18 of leaf water: A crossroad for plant associated isotopic signal, in *Stable Isotopes: Integration of Biological, Ecological and Geochemical Processes*, edited by H. Griffiths, pp. 147–168, BIOS Sci., Oxford, U.K.

Yakir, D., and L. S. L. Sternberg (2000), The use of stable isotopes to study ecosystem gas exchange, *Oecologia*, *123*, 297–311.

Yakir, D., and X. F. Wang (1996), Fluxes of CO_2 and water between terrestrial vegetation and the atmosphere estimated from isotope measurements, *Nature*, *380*, 515–517.

Zencich, S. J., R. H. Froend, and J. V. Turner (2002), Influence of groundwater depth on the seasonal sources of water accessed by Banksia tree species on a shallow sandy coastal aquifer, *Oecologia*, *131*, 8–19.

K. Kim and X. Lee, School of Forestry and Environmental Studies, Yale University, 21 Sachem Street, New Haven, CT 06511, USA. (xuhui.lee@yale.edu)

R. Smith, Department of Geology and Geophysics, Yale University, New Haven, CT 06520, USA.